Technical Note: Multipurpose CT, ultrasound, and MRI breast phantom for use in radiotherapy and minimally invasive interventions

Mark Ruschin[a)]
Department of Medical Physics, Sunnybrook Odette Cancer Centre, Toronto, Ontario M4N 3M5, Canada and Department of Radiation Oncology, University of Toronto, Toronto, Ontario M4N 3M5, Canada

Sean R. H. Davidson
Techna Institute, University Health Network, Toronto, Ontario M5G 1P5, Canada

William Phounsy
Department of Physics, Ryerson University, Toronto, Ontario M5B 2K3, Canada

Tae Sun Yoo
Institute of Health Policy, University of Toronto, Toronto, Ontario M5T 3M6, Canada

Lee Chin
Department of Medical Physics, Sunnybrook Odette Cancer Centre, Toronto, Ontario M4N 3M5, Canada and Department of Radiation Oncology, University of Toronto, Toronto, Ontario M4N 3M5, Canada

Jean-Philippe Pignol
Department of Radiation Oncology, Erasmus MC Cancer Institute, 3075 EA Rotterdam, Netherlands

Ananth Ravi and Claire McCann
Department of Medical Physics, Sunnybrook Odette Cancer Centre, Toronto, Ontario M4N 3M5, Canada and Department of Radiation Oncology, University of Toronto, Toronto, Ontario M4N 3M5, Canada

(Received 27 November 2015; revised 1 April 2016; accepted for publication 5 April 2016; published 26 April 2016)

Purpose: To develop a multipurpose gel-based breast phantom consisting of a simulated tumor with realistic imaging properties in CT, ultrasound and MRI, or a postsurgical cavity on CT. Applications for the phantom include: deformable image registration (DIR) quality assurance (QA), autosegmentation validation, and localization testing and training for minimally invasive image-guided procedures such as those involving catheter or needle insertion.
Methods: A thermoplastic mask of a typical breast patient lying supine was generated and then filled to make an array of phantoms. The background simulated breast tissue consisted of 32.4 g each of ballistic gelatin (BG) powder and Metamusil™ (MM) dissolved in 800 ml of water. Simulated tumors were added using the following recipe: 12 g of barium sulfate (1.4% v/v) plus 0.000 14 g copper sulfate plus 0.7 g of MM plus 7.2 g of BG all dissolved in 75 ml of water. The phantom was evaluated quantitatively in CT by comparing Hounsfield units (HUs) with actual breast tissue. For ultrasound and MRI, the phantoms were assessed based on subjective image quality and signal-difference to noise (SDNR) ratio, respectively. The stiffness of the phantom was evaluated based on ultrasound elastography measurements to yield an average Young's modulus. In addition, subjective tactile assessment of phantom was performed under needle insertion.
Results: The simulated breast tissue had a mean background value of 24 HU on CT imaging, which more closely resembles fibroglandular tissue (40 HU) as opposed to adipose (−100 HU). The tumor had a mean CT number of 45 HU, which yielded a qualitatively realistic image contrast relative to the background either as an intact tumor or postsurgical cavity. The tumor appeared qualitatively realistic on ultrasound images, exhibiting hypoechoic characteristics compared to background. On MRI, the tumor exhibited a SDNR of 3.7. The average Young's modulus was computed to be 15.8 ± 0.7 kPa (1 SD).
Conclusions: We have developed a process to efficiently and inexpensively produce multipurpose breast phantoms containing simulated tumors visible on CT, ultrasound, and MRI. The phantoms have been evaluated for image quality and elasticity and can serve as a medium for DIR QA, autosegmentation QA, and training for minimally invasive procedures. [http://dx.doi.org/10.1118/1.4947124]

Key words: breast phantom, deformable image registration, radiotherapy, brachytherapy, radiofrequency ablation, imaging, gel

1. INTRODUCTION

Adjuvant whole breast irradiation (WBI) following breast conserving surgery (BCS) has been demonstrated to improve local control and reduce breast cancer mortality.[1,2] Despite a reduction in radiation-induced side effects brought about through the use of IMRT, the rate of acute toxicity resulting from WBI is relatively high with Grade 2 or higher acute skin toxicity (National Cancer Institute Common Toxicity Criteria Scale[3]) occurring in around 30% of patients depending on the technique.[4] To potentially improve treatment tolerance, minimally invasive techniques are being investigated to manage early-stage breast cancer including radiofrequency ablation (RFA)[5–9] of the intact tumor, or brachytherapy,[10–12] or partial breast irradiation (PBI) of postsurgical bed.[13,14]

For minimally invasive interventions such as RFA or brachytherapy, the ability to perform image guidance to accurately localize the target is essential. CT images are often used for external beam and brachytherapy planning, whereas RFA relies on accurate placement of a device into the tumor, which can be accomplished via real-time ultrasound image guidance. The role of MRI is also being explored in terms of target delineation and localization for minimally invasive procedures, as well as in emerging technologies such as the MRI-linac.[15–17] Therefore, a phantom that could be used across multiple imaging modalities could address the localization testing needs of radiotherapy, RFA, and other minimally invasive procedures, as well as evaluate novel treatments generated from emerging technologies and multimodality therapies. The ideal phantom would permit both post-tumor resection and intact tumor treatment conditions, with the latter containing a target representing a tumor that is visible on all imaging modalities. The ideal phantom would also possess realistic bulk material properties in order to test physical deployment of needles or catheters, as well as to simulate deformation.

Since the breast is a highly mobile and deformable organ, daily deformable image registration (DIR) between the treated anatomy and the planned anatomy is required.[18] The successful implementation of DIR into radiation oncology has been hindered by a lack of available quality assurance (QA) and validation tools.[19] For conformal breast irradiation, such tools are necessary to fully leverage adaptive planning techniques.[20] The current literature suggests that site-specific DIR validation be performed using phantoms with clinically relevant image contrast for the site of interest.[19,21] For breast, the need for DIR validation is primarily driven by the interest in PBI and even for conformal boost (sequential or simultaneous integrated) with the published data indicating substantial interfraction mobility of the breast.[18,22] The recent publication of the external beam RAPID study indicates adverse cosmesis and late toxicity compared to whole breast irradiation may further motivate the need to reduce the volume of treated tissue via online DIR and adaptive radiotherapy approach.[23]

Finally, given the trend toward multimodality treatment using minimally invasive techniques, a phantom that permits volumetric treatment preplanning (for radio and thermal therapy) and serves as a tool for training minimally invasive techniques under real-time image guidance was developed. To ensure ease of use and handling, low cost, anatomical accuracy and compatibility with all imaging modalities, a phantom made of gel, a surrogate for human tissue, was developed.[24] The purpose of this study then was to develop a gel-based multimodality breast phantom that enables QA and provides a means for training in the context of minimally invasive techniques.

2. METHODS

2.A. Breast phantom development

2.A.1. Inverse mold preparation

Plastic or Styrofoam molds were machined from CT scans of breast patients lying supine in treatment position. A thermoplastic mask (ORFIT) was then tightly fitted around the mold creating a hollow or "inverse" mold that was subsequently filled with the phantom mixture to generate the gel-based phantoms. This process of inverse mold generation based on real patient CT scans allows for the generation of different shapes and sizes of breast phantoms, as illustrated in Fig. 1. Machining a single positive mold allowed us to inexpensively create multiple inverse molds, which in turn allowed mixing and pouring of multiple molds at the same time. Machining multiple inverse molds directly would have been substantially more expensive.

2.A.2. Background simulated breast

For a medium-sized breast, the volume of an inverse mold is typically 800 ml. To determine the appropriate gelatin (Vyse, Schiller Park, IL) concentration, phantoms were generated with increasing gelatin concentration.[25,26] The minimum concentration that produced a stable phantom (i.e.,

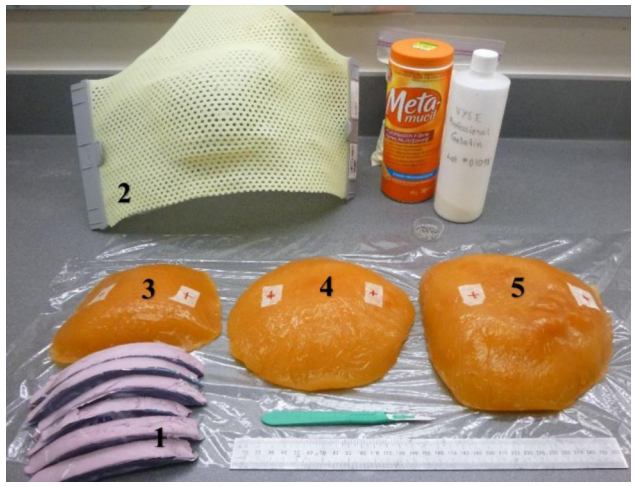

FIG. 1. Construction of breast phantoms. (1) Slices of Styrofoam mold generated from a CT scan of a patient. (2) An inverse mold created based on the Styrofoam mold. (3)–(5) Different gel-based phantoms corresponding to a small, medium, and large breast.

one that did not tear easily when deformed) was 32.4 g powder per 800 ml water (4.05% by weight).

For ultrasound imaging contrast, a simple low-cost technique was adopted from the literature in which a sugar-free psyllium hydrophilic mucilloid fiber [brand name: sugar-free Metamucil (MM)] is used as the scattering medium.[27] A photo of some sample phantoms is shown in Fig. 1.

2.A.3. Simulated tumor

In order to embed a simulated tumor into the breast phantom, a portion of the breast phantom in its semi-colloidal phase (approximately 45 min at 1–4 °C) is scooped out and filled with an experimentally determined solution consisting of $BaSO_4$ powder for CT contrast and $CuSO_4$ for MRI contrast, as detailed in Table I(a). Ultrasound contrast arises due to the lower concentration of MM in the simulated tumor compared to the background simulated breast tissue. On CT, the image contrast of intact tumors or postsurgical cavities is similar in our experience, whereas for MRI and ultrasound, the present phantom only represents intact tumor. This solution is injected into the scooped-out region, leaving some room that is filled with background breast tissue material after the tumor material has had a chance to set. Aluminum markers approximately 1 mm in diameter (commonly referred to as "BB"s in radiotherapy clinics) can also be implanted in the simulated tumors to serve as fiducials for DIR evaluation. These small markers can be digitally subtracted from any image (reference or physically deformed)[28] and their voxels tracked to serve as surrogates for DIR accuracy without affecting the quality of the DIR itself. The entire process of producing a batch of phantoms is approximately 20 min for mixing and several hours to set.

2.B. Breast phantom properties

2.B.1. CT

CT images of breast phantoms were acquired on a Brilliance Big Bore scanner (Philips Medical Systems, Cleveland, USA) using the institution's breast planning protocol, which consists of a 2 mm slice thickness, 120 kVp, and 400 mAs. The mean and standard deviation of the CT number in the background and in the simulated tumor was measured and compared to published and in-house data of breast patients. The CT contrast of the tumor or cavity relative to the background was rated by an experienced breast radiation oncologist (J.P) as simply "yes—realistic contrast" or "no—unrealistic contrast" in approximately 20 phantoms generated over the course of the present project. Other imaging features such as texture were not evaluated, as texture is not relevant for our purpose and applications.

TABLE I(a). Finalized material characteristics of phantom. BG = Ballistics gel. MM = Metamucil.

	Water	Contrast media
Background breast	800 ml	BG (32.4 g) + MM (32.4 g)
Tumor	75 ml	BG (7.2 g) + MM (0.7 g) + $BaSO_4$ (12 ml) + $CuSO_4$ (0.000 14 g)

2.B.2. MRI

MR images of the breast phantoms were acquired on an Achieva 3T MRI scanner (Philips Medical Systems, Cleveland, USA) using a 3D T1-weighted Fast-Field Echo sequence, with the phantom placed in an 8-channel head coil. The reconstruction matrix was $240\times240\times208$ with a voxel size of $0.96\times0.96\times0.94$ mm. We also acquired coronal view T2-weighted images using Turbo-Spin Echo. The phantom image was compared to a real breast cancer image, acquired on a Signa HDxt 1.5T MRI scanner (GE Healthcare, Milwaukee, USA) using the T1-weighted VIBRANT protocol with fat suppression. At our institution, patients are often scanned in prone position, using a dedicated breast coil, whereas the phantom was scanned supine. The signal-difference-to-noise ratio (SDNR) between tumor and background was measured for a simulated phantom and a breast patient using T1-weighted images. In one phantom, the MRI contrast of the tumor relative to the background was rated by an experienced breast radiation oncologist (J.P) as simply yes—realistic contrast or no—unrealistic contrast. Other imaging features such as texture were not evaluated as texture is not relevant for our purpose and applications.

2.B.3. Ultrasound and mechanical

Ultrasound images of the breast phantoms were acquired using a Sonosite Titan ultrasound imaging system (Bothell, WA, USA). Ultrasound images of 5 phantoms were evaluated qualitatively by radiation oncologists with over 5 yr of clinical experience performing ultrasound-guided postsurgical brachytherapy as either "yes—realistic image" or "no—unrealistic image." The Young's modulus was also estimated using ultrasound-based elastography on a Supersonic Imagine Aixplorer (Aixplorer; SuperSonic Imagine SA, Aix-en-Provence, France) with a L15-4 linear array transducer using the "breast" preset. The central frequency was not explicitly given but estimated to be in the 7–10 MHz range. The elastography experiments consisted of single measurements in four different phantoms, each made from a different batch of phantom material. The data were averaged over a circular area of 13 mm diameter centered at a depth of about 2.4 cm from the surface using the shear wave technique described in detail by Bercoff *et al.*[29]

The phantom was also evaluated for its tactile properties. The handling of the phantom and the placement of brachytherapy catheters into the phantom by the same experienced radiation oncologist in a mock brachytherapy procedure was used to assess the physical realism of the phantom. This subjective evaluation consisted of "yes—realistic feel" or "no—unrealistic feel" in 5 phantoms. The integrity of the phantom was assessed during the mock brachytherapy procedure by examining the phantom for the presence of tears.

TABLE I(b). Measured properties of breast phantom. SDNR = Signal difference to noise ratio.

Property	Observed mean values (standard deviation)	Expected values (range)	Source
CT number: background	+24 HU (SD ± 9 HU)	−100 HU (adipose) to +40 HU (fibroglandular)	Refs. 30 and 31
CT number: tumor/cavity	+45 HU (SD ± 8 HU)	+40 to +60 HU	In-house (n = 10)
SDNR on T1 MRI	20	60–70	In-house (n = 1)
Young's modulus	15.8 kPa (SD ± 0.7 kPa)	7 kPa (adipose) to 30–50 kPa (breast parenchyma)	Ref. 32

3. RESULTS

The various measured properties of the breast phantom are summarized in Table I(b), and representative images of the phantom alongside patient images are shown in Fig. 2.

The measured mean CT number of 24 Hounsfield units (HU) in the breast phantom background reflects a density similar to fibroglandular breast tissue.[30,31] The measured mean CT number of the tumor was 45 HU, which is within the range of values of what we observed in 5 breast cancer patients with intact tumors and 5 patients with postsurgical cavities. Despite the high density of the phantom background, the CT image contrast between the tumor and the background in the phantom was deemed "realistic" in all 20 phantoms shown to a radiation oncologist. As shown in Fig. 3, implanted aluminum markers were digitally removed, resulting in image profiles with the characteristics of the surrounding medium.

The contrast of the simulated tumor on MRI was deemed realistic by a radiation oncologist and subjectively appears similar to a clinical case as shown in Figs. 2(c) and 2(d).

The ultrasound images of the simulated tumor showed hypoechoic qualities and were deemed realistic in 5 cases by the radiation oncologist, an example of which is shown in Fig. 2(f) alongside a real tumor in Fig. 2(e). The mean measured Young's modulus of the phantom was 15.8 kPa, which is in the range of published values.[32] Furthermore, the tactility of the phantom (i.e., "the feel of the phantom")

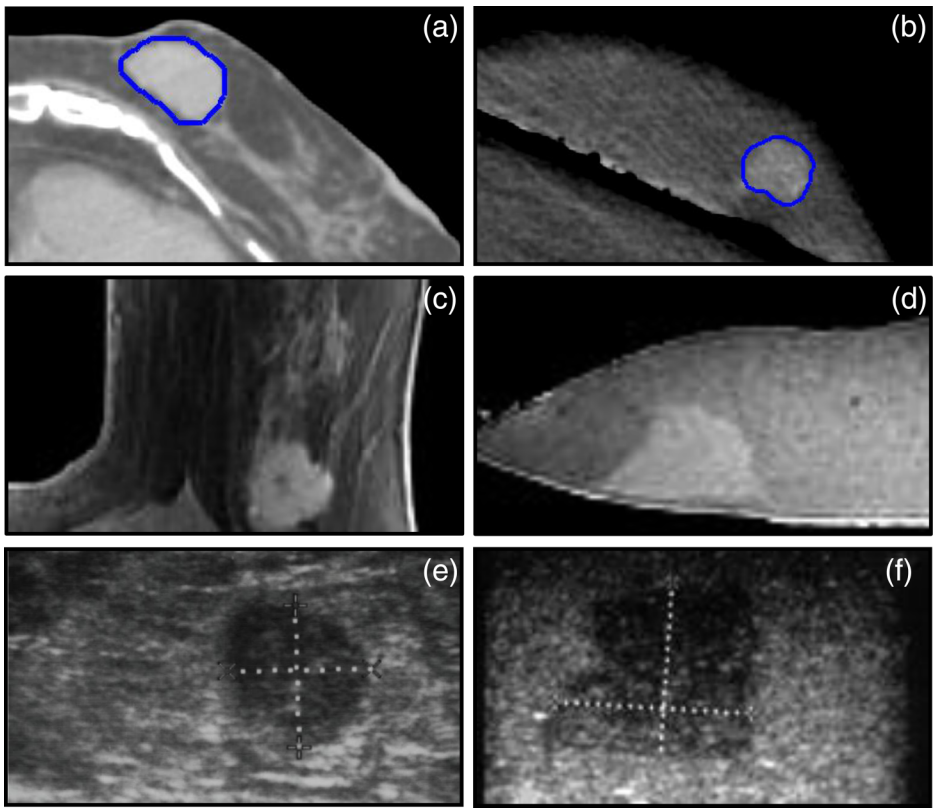

FIG. 2. Sample images of real and phantom breast exhibiting tumors. (a) CT image of breast patient with tumor outlined in dark blue; (b) CT image of breast phantom with simulated tumor outline in dark blue; (c) T1-weighted MRI of breast patient with T1N0 ductal carcinoma; (d) T1-weighted image of breast phantom; (e) ultrasound image of same breast patient as in (c), showing hypoechoic tumor; (f) ultrasound image of breast phantom showing hypoechoic simulated tumor. Please note that the CT image in (a) belongs to a different patient than in parts (c) and (e) since all three modalities are rarely used in parallel. (See color online version.)

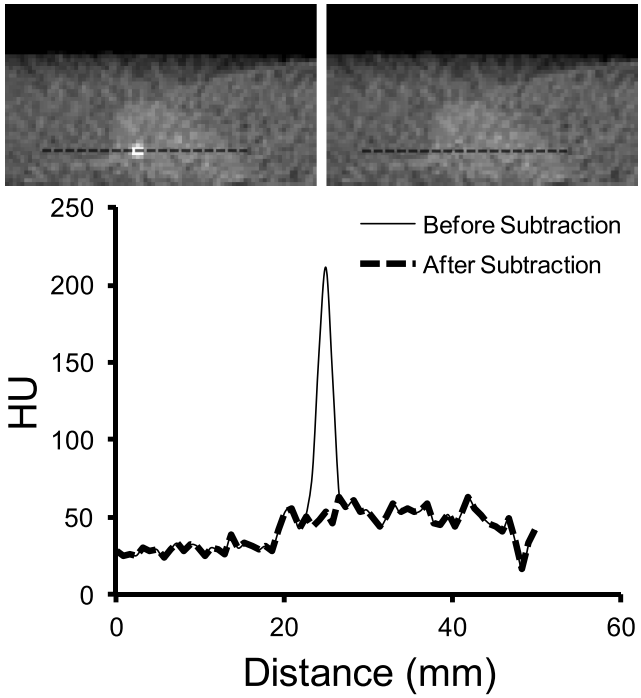

FIG. 3. Example of digital subtraction of aluminum marker from CT image of breast phantom. The aluminum marker is shown in the upper left as a small white sphere embedded in a simulated tumor. The black dashed line indicates the line profile taken across the CT image before and after marker subtraction and plotted in bottom graph.

was deemed realistic by a radiation oncologist with dedicated breast experience. As shown in Fig. 4, the integrity of the breast phantom was maintained throughout catheter insertions in a mock brachytherapy setup.

FIG. 4. Brachytherapy catheter insertion in breast phantom.

4. DISCUSSION

The present work focuses on the development of a multimodality and low cost breast phantom for testing, evaluation, and planning of radiotherapy and minimally invasive procedures such as RFA or brachytherapy. The results of the study indicate that the phantom is compatible with CT, MRI, and Ultrasound. Simulation of a breast with an intact tumor with realistic imaging properties was developed for evaluation of DIR and for training individuals on how to perform the minimally invasive procedures.

CT images show that the phantom resembled breast tissue that was primarily fibroglandular.[30,31] The image contrast of the tumor-mimicking insert was qualitatively characteristic of a real tumor, although the CT number of the tumor is somewhat higher than in a real patient. For the purposes of delineation for planning and training, however, the contrast of the simulated tumor was reasonable. Implanted aluminum markers were also clearly visible on CT and could be used to quantify DIR algorithms without biasing the results of the DIR itself, using the digital subtraction method. Although there was limited clinical MRI data available for comparison, the image contrast of the simulated tumor on T1-weighted images also resembled that of a real breast cancer patient. On both CT and MRI, textural detail of adipose and fibroglandular tissue in a real breast can be visualized, whereas the breast phantom surrounding the simulated tumor was completely uniform, which for localization testing and tumor DIR is sufficient. Ultrasound images showed the hypoechoic features of the simulated tumor, which closely resembled those of a real breast cancer patient, making the phantom highly suitable for ultrasound-based real-time image guidance of minimally invasive procedures. The Young's modulus of the phantom was found to be similar to the Young's modulus of adipose and fibroglandular tissues.[32] Subjectively, the expert breast radiation oncologist considered the phantom to feel like a real breast and appropriate for the purposes of training and quality assurance.

One potential drawback of the phantom is that it should be used within a week or two of fabrication. The phantom must be stored in a refrigerator and wrapped in cellophane when not being used to prevent it from drying and cracking. Depending on the test, the phantom is typically manufactured for one-time use only, for example, testing the targeting accuracy of an interventional technique such as RFA or brachytherapy. However, the simplicity and low cost of the manufacturing process in addition to the multimodality functionality mitigate the one-time use limitation of this phantom. One may also argue that another limitation of the current phantom design is the lack of reproducibility in the positioning of the simulated tumor. For target localization accuracy testing, however, the position of the simulated tumor was identified in imaging and as such, there was limited value in positional accuracy in between localization experiments.

The present phantom could be easily used to evaluate DIR algorithms. A major advantage of the phantom for DIR QA is that numerous phantoms with numerous tumors can be generated, each with unique size and shapes. This feature

overcomes a particular limitation of existing phantoms that are fixed in size and shape and therefore may not fully test a range of possible clinical scenarios encountered with DIR. However, for routine QA of DIR algorithms over time or across institutions, it would be beneficial to construct a phantom with reproducible characteristics, which is the subject of ongoing work. Furthermore, since the initial intent was to perform all deformation imaging in one session, we did not consider the deformation reproducibility over time or as a function of temperature. Commercial phantoms include those by CIRS but these are limited in the number of times they can be used and also do not include fiducials. The gel-based phantom presented by Yeo *et al.* is similar in philosophy to the phantom in the present work but is not specific to the breast geometry and is not ultrasound-compatible.[28] Future work involves developing the phantom recipe further to include dosimetric gels in order to perform end-to-end testing and validate dose distributions derived from emerging technologies such as the MRI–Linac.[17,33,34]

5. CONCLUSION

The present study describes a breast phantom that is suitable for multiple purposes in the context of radiotherapy and RFA using CT, MRI, and ultrasound image guidance. Multimodality treatment approaches such as brachytherapy, RFA, and radiotherapy would largely benefit from such an integrated and cost-effective phantom.

ACKNOWLEDGMENTS

The authors would like to acknowledge the help of Ross Williams and Dr. Peter Burns at the Sunnybrook Research Institute for their assistance with the U.S. elastography measurements. The authors also would like to thank Samuel Richardo at the Sunnybrook Research Institute for his help in performing MRI scans of the phantom.

[a]Author to whom correspondence should be addressed. Electronic mail: Mark.Ruschin@sunnybrook.ca

[1]Canadian Cancer Society's Steering Committee on Cancer Statistics, *Canadian Cancer Statistics* (Canadian Cancer Society, Toronto, ON, 2012).

[2]M. Quan, N. Hodgson, R. Przybysz, N. Gunraj, S. Schultz, N. Baxter, D. Urbach, and M. Simunovic, "Surgery for breast cancer," in *Cancer Surgery in Ontario: ICES Atlas*, edited by D. R. Urbach, M. Simunovic, and S. E. Schultz (Institute for Clinical Evaluative Sciences, Toronto, 2008).

[3]Common Terminology Criteria for Adverse Events (CTCAE) Version 4.03, U.S. Department of Health and Human Services, National Insitutes of Health and National Cancer Institute, 2010.

[4]J. P. Pignol, I. Olivotto, E. Rakovitch, S. Gardner, K. Sixel, W. Beckham, T. T. Vu, P. Truong, I. Ackerman, and L. Paszat, "A multicenter randomized trial of breast intensity-modulated radiation therapy to reduce acute radiation dermatitis," J. Clin. Oncol. **26**, 2085–2092 (2008).

[5]B. A. Grotenhuis, W. W. Vrijland, and T. M. Klem, "Radiofrequency ablation for early-stage breast cancer: Treatment outcomes and practical considerations," Eur. J. Surg. Oncol. **39**, 1317–1324 (2013).

[6]A. H. Hayashi, S. F. Silver, N. G. van der Westhuizen, J. C. Donald, C. Parker, S. Fraser, A. C. Ross, and I. A. Olivotto, "Treatment of invasive breast carcinoma with ultrasound-guided radiofrequency ablation," Am. J. Surg. **185**, 429–435 (2003).

[7]M. Kontos, E. Felekouras, and I. S. Fentiman, "Radiofrequency ablation in the treatment of primary breast cancer: No surgical redundancies yet," Int. J. Clin. Pract. **62**, 816–820 (2008).

[8]S. Oura, T. Tamaki, I. Hirai, T. Yoshimasu, F. Ohta, R. Nakamura, and Y. Okamura, "Radiofrequency ablation therapy in patients with breast cancers two centimeters or less in size," Breast Cancer **14**, 48–54 (2007).

[9]N. Yamamoto, H. Fujimoto, R. Nakamura, M. Arai, A. Yoshii, S. Kaji, and M. Itami, "Pilot study of radiofrequency ablation therapy without surgical excision for T1 breast cancer: Evaluation with MRI and vacuum-assisted core needle biopsy and safety management," Breast Cancer **18**, 3–9 (2011).

[10]C. Polgár, J. Fodor, T. Major, G. Németh, K. Lövey, Z. Orosz, Z. Sulyok, Z. Takácsi-Nagy, and M. Kásler, "Breast-conserving treatment with partial or whole breast irradiation for low-risk invasive breast carcinoma–5-year results of a randomized trial," Int. J. Radiat. Oncol., Biol., Phys. **69**, 694–702 (2007).

[11]D. E. Wazer, S. Kaufman, L. Cuttino, T. DiPetrillo, and D. W. Arthur, "Accelerated partial breast irradiation: An analysis of variables associated with late toxicity and long-term cosmetic outcome after high-dose-rate interstitial brachytherapy," Int. J. Radiat. Oncol., Biol., Phys. **64**, 489–495 (2006).

[12]J. P. Pignol, J. M. Caudrelier, J. Crook, C. McCann, P. Truong, and H. A. Verkooijen, "Report on the clinical outcomes of permanent breast seed implant for early-stage breast cancers," Int. J. Radiat. Oncol., Biol., Phys. **93**, 614–621 (2015).

[13]L. Livi, F. B. Buonamici, G. Simontacchi, V. Scotti, M. Fambrini, A. Compagnucci, F. Paiar, S. Scoccianti, S. Pallotta, B. Detti, B. Agresti, C. Talamonti, M. Mangoni, S. Bianchi, L. Cataliotti, L. Marrazzo, M. Bucciolini, and G. Biti, "Accelerated partial breast irradiation with IMRT: New technical approach and interim analysis of acute toxicity in a phase III randomized clinical trial," Int. J. Radiat. Oncol., Biol., Phys. **77**, 509–515 (2010).

[14]A. G. Taghian, K. R. Kozak, K. P. Doppke, A. Katz, B. L. Smith, M. Gadd, M. Specht, K. Hughes, K. Braaten, L. A. Kachnic, A. Recht, and S. N. Powell, "Initial dosimetric experience using simple three-dimensional conformal external-beam accelerated partial-breast irradiation," Int. J. Radiat. Oncol., Biol., Phys. **64**, 1092–1099 (2006).

[15]K. H. Ahn, B. A. Hargreaves, M. T. Alley, K. C. Horst, G. Luxton, B. L. Daniel, and D. Hristov, "MRI guidance for accelerated partial breast irradiation in prone position: Imaging protocol design and evaluation," Int. J. Radiat. Oncol., Biol., Phys. **75**, 285–293 (2009).

[16]J. Godinez, E. C. Gombos, S. A. Chikarmane, G. K. Griffin, and R. L. Birdwell, "Breast MRI in the evaluation of eligibility for accelerated partial breast irradiation," AJR, Am. J. Roentgenol. **191**, 272–277 (2008).

[17]C. Kontaxis, G. H. Bol, J. J. Lagendijk, and B. W. Raaymakers, "Towards adaptive IMRT sequencing for the MR-linac," Phys. Med. Biol. **60**, 2493–2509 (2015).

[18]A. van Mourik, S. van Kranen, S. den Hollander, J. J. Sonke, M. van Herk, and C. van Vliet-Vroegindeweij, "Effects of setup errors and shape changes on breast radiotherapy," Int. J. Radiat. Oncol., Biol., Phys. **79**, 1557–1564 (2011).

[19]K. Nie, C. Chuang, N. Kirby, S. Braunstein, and J. Pouliot, "Site-specific deformable imaging registration algorithm selection using patient-based simulated deformations," Med. Phys. **40**, 041911 (10pp.) (2013).

[20]E. E. Ahunbay, J. Robbins, R. Christian, A. Godley, J. White, and X. A. Li, "Interfractional target variations for partial breast irradiation," Int. J. Radiat. Oncol., Biol., Phys. **82**, 1594–1604 (2012).

[21]N. Kirby, C. Chuang, U. Ueda, and J. Pouliot, "The need for application-based adaptation of deformable image registration," Med. Phys. **40**, 011702 (10pp.) (2013).

[22]Y. Hasan, L. Kim, J. Wloch, Y. Chi, J. Liang, A. Martinez, D. Yan, and F. Vicini, "Comparison of planned versus actual dose delivered for external beam accelerated partial breast irradiation using cone-beam CT and deformable registration," Int. J. Radiat. Oncol., Biol., Phys. **80**, 1473–1476 (2011).

[23]I. A. Olivotto, T. J. Whelan, S. Parpia, D. H. Kim, T. Berrang, P. T. Truong, I. Kong, B. Cochrane, A. Nichol, I. Roy, I. Germain, M. Akra, M. Reed, A. Fyles, T. Trotter, F. Perera, W. Beckham, M. N. Levine, and J. A. Julian, "Interim cosmetic and toxicity results from RAPID: A randomized trial of accelerated partial breast irradiation using three-dimensional conformal external beam radiation therapy," J. Clin. Oncol. **31**, 4038–4045 (2013).

[24]N. Niebuhr, W. Johnen, T. Güldaglar, A. Runz, G. Echner, P. Mann, C. Möhler, A. Pfaffenberger, O. Jäkel, and S. Greilich, "Technical note: Radiological properties of tissue surrogates used in a multimodalitydeformable pelvic phantom for MR-guided radiotherapy," Med. Phys. **43**, 908–916 (2016).

[25]M. L. Fackler and J. A. Malinowski, "Ordnance gelatin for ballistic studies. Detrimental effect of excess heat used in gelatin preparation," Am. J. Forensic Med. Pathol. **9**, 218–219 (1988).
[26]K. B. Reed, A. M. Okamura, and N. J. Cowan, "Controlling a robotically steered needle in the presence of torsional friction," in *IEEE International Conference on Robotics and Automation* (IEEE, Kobe, 2009), pp. 3476–3481.
[27]R. O. Bude and R. S. Adler, "An easily made, low-cost, tissue-like ultrasound phantom material," J. Clin. Ultrasound **23**, 271–273 (1995).
[28]U. J. Yeo, J. R. Supple, M. L. Taylor, R. Smith, T. Kron, and R. D. Franich, "Performance of 12 DIR algorithms in low-contrast regions for mass and density conserving deformation," Med. Phys. **40**, 101701 (12pp.) (2013).
[29]J. Bercoff, M. Tanter, and M. Fink, "Supersonic shear imaging: A new technique for soft tissue elasticity mapping," IEEE Trans. Ultrason., Ferroelectr., Freq. Control **51**, 396–409 (2004).
[30]D. R. White, R. J. Martin, and R. Darlison, "Epoxy resin based tissue substitutes," Br. J. Radiol. **50**, 814–821 (1977).
[31]International Commission on Radiation Units and Measurements, "Tissue substitutes in radiation dosimetry and measurements," International Commission on Radiation Units and Measurements Report No. 44, 1989.
[32]A. Athanasiou, A. Tardivon, M. Tanter, B. Sigal-Zafrani, J. Bercoff, T. Deffieux, J. L. Gennisson, M. Fink, and S. Neuenschwander, "Breast lesions: Quantitative elastography with supersonic shear imaging–preliminary results," Radiology **256**, 297–303 (2010).
[33]S. R. Mahdavi, A. D. Esmaeeli, M. Pouladian, A. S. Monfared, D. Sardari, and S. Bagheri, "Breast dosimetry in transverse and longitudinal field MRI-linac radiotherapy systems," Med. Phys. **42**, 925–936 (2015).
[34]T. C. van Heijst, M. D. den Hartogh, J. J. Lagendijk, H. J. van den Bongard, and B. van Asselen, "MR-guided breast radiotherapy: Feasibility and magnetic-field impact on skin dose," Phys. Med. Biol. **58**, 5917–5930 (2013).